Growth of spinodal instabilities in nuclear matter. II. Asymmetric matter

F. Acar,[1] S. Ayik,[2,*] O. Yilmaz,[1,†] and A. Gokalp[3]

[1]*Physics Department, Middle East Technical University, 06800 Ankara, Turkey*
[2]*Physics Department, Tennessee Technological University, Cookeville, Tennessee 38505, USA*
[3]*Department of Physics, Bilkent University, 06800 Ankara, Turkey*

As an extension of our previous work, the growth of density fluctuations in the spinodal region of charge asymmetric nuclear matter is investigated in the basis of the stochastic mean-field approach in the nonrelativistic framework. A complete treatment of density correlation functions is presented by including collective modes and noncollective modes.

PACS number(s): 24.60.Ky, 25.70.Pq, 25.75.Gz

I. INTRODUCTION

Nuclear matter in the spinodal region exhibits a universal behavior. When the uniform matter enters into the spinodal region, small fluctuations grow rapidly and the matter undergoes a dynamical liquid-gas phase transformation. Nuclear multifragmentation processes are considered as a signature for such a dynamical phase transformation in nuclear matter [1–3]. Theoretical description of the spinodal dynamics requires an approach beyond the mean-field theory by incorporating fluctuation mechanisms [4–7]. The recently proposed stochastic mean-field approach (SMF) provides a useful framework for describing large amplitude nuclear collective motion by including one-body dissipation and fluctuation mechanisms [8]. We carried out a number of investigations of the spinodal instabilities by employing the nonrelativistic and relativistic framework of the SMF approach [9–13]. For a full description of the spinodal dynamics, we need to determine an ensemble of events by simulating the SMF equation with proper fluctuations in the initial state. In our investigation, instead of such simulations, we calculate the early growth of density fluctuations in the linear response regime of the SMF approach. For this purpose, the equal time correlation function of the density fluctuations provides a very useful quantity. For nuclear matter, in the linear response regime, it is possible to provide a nearly analytical treatment for the density correlation function. Indeed, the density correlation function exhibits the early stages of the dynamics of the liquid-gas phase transformation. In our earlier studies, we calculated the correlation function in the pole approximation. As pointed out by Bozek, the effect of noncollective poles play an important role in the full description of the correlation function [14]. In a recent work, we calculated the density correlation function exactly by including the effects of noncollective poles in addition to the collective poles for charge symmetric nuclear matter [15]. In this work, we present calculations of the density correlation function for charge asymmetric nuclear matter in the semiclassical framework, i.e., in the long wavelength limit, of the SMF approach. In Sec. II, we briefly present description

of the density correlation functions including collective and noncollective modes in the linear response framework in the long wavelength limit. In Sec. III, we present calculations for the most unstable initial density $\rho = 0.3\rho_0$ at two different temperatures and two charge asymmetries of the matter. Conclusions are given in Sec. IV.

II. DENSITY CORRELATION FUNCTIONS IN ASYMMETRIC NUCLEAR MATTER

A detailed description of the correlation function of the density fluctuations for symmetric matter including the noncollective poles is presented in our recent publication [15]. A description of the correlation function for the charge asymmetric system is given in a similar manner. Here, we give a brief description and refer to Refs. [9,15] for details. For the charge asymmetric case, we need to consider the coupled SMF equations for neutrons and protons. The linearized equations for fluctuations of neutron and proton density matrices, $\delta\hat{\rho}_a^\lambda(t) = \hat{\rho}_a^\lambda(t) - \hat{\rho}_a$, are given by

$$i\hbar\frac{\partial}{\partial t}\delta\hat{\rho}_a^\lambda(t) = \left[h_a, \delta\hat{\rho}_a^\lambda(t)\right] + \left[\delta U_a^\lambda(t), \hat{\rho}_a\right], \quad (1)$$

where $\hat{\rho}_a$ is the density matrix of the initial state, h_a denotes the mean-field Hamiltonian in the initial state, and δU_a^λ is the fluctuating part of the mean field for protons and neutrons $a = p$ and n in the event labeled by λ. Because for infinite matter the equilibrium state and the mean-field Hamiltonian are homogeneous, it is suitable to analyze these equations in plane wave representations. Then, the linear response equation becomes

$$i\hbar\frac{\partial}{\partial t}\langle\vec{p}_1|\delta\hat{\rho}_a^\lambda(t)|\vec{p}_2\rangle = [\varepsilon_a(\vec{p}_1) - \varepsilon_a(\vec{p}_2)]\langle\vec{p}_1|\delta\hat{\rho}_a^\lambda(t)|\vec{p}_2\rangle$$
$$- [\rho_a(\vec{p}_1) - \rho_a(\vec{p}_2)]\langle\vec{p}_1|\delta U_a^\lambda(t)|\vec{p}_2\rangle. \quad (2)$$

The space Fourier transform of nucleon density fluctuations $\delta\rho^\lambda(\vec{k},t)$ is related to the fluctuations of the density matrix according to

$$\delta\rho_a(\vec{k},t) = \sum_s \int \frac{d^3p}{(2\pi\hbar)^3}\langle\vec{p} + \hbar\vec{k}/2|\delta\hat{\rho}_{a,s}(t)|\vec{p} - \hbar\vec{k}/2\rangle, \quad (3)$$

*ayik@tntech.edu
†oyilmaz@metu.edu.tr

where the summation indicates the sum over spin quantum number $s = \uparrow, \downarrow$. We solve the linear response Eq. (2) by employing the method of one-sided Fourier transformation in

time [16,17] and obtain coupled algebraic equations for the Fourier transform of the local proton and neutron densities $\delta \rho_a^\lambda(\vec{k}, \omega)$:

$$
\begin{pmatrix} [1 + F_0^{nn} \chi_n(\vec{k}, \omega)] \delta \rho_n^\lambda(\vec{k}, \omega) + F_0^{np} \chi_n(\vec{k}, \omega) \delta \rho_p^\lambda(\vec{k}, \omega) \\ [1 + F_0^{pp} \chi_p(\vec{k}, \omega)] \delta \rho_p^\lambda(\vec{k}, \omega) + F_0^{pn} \chi_p(\vec{k}, \omega) \delta \rho_n^\lambda(\vec{k}, \omega) \end{pmatrix} = i \begin{pmatrix} S_n^\lambda(\vec{k}, \omega) \\ S_p^\lambda(\vec{k}, \omega) \end{pmatrix}.
\tag{4}
$$

In deriving these coupled equations, we consider that the mean-field potential depends only on the local nucleon densities, $U_a^\lambda = U(\rho_p^\lambda, \rho_n^\lambda)$. The source term $S_a^\lambda(\vec{k}, \omega)$ is determined by the matrix elements of fluctuations of the initial density matrix $\delta \hat{\rho}_{a,s}^\lambda(0)$ in the spin-isospin channel as

$$
S_a^\lambda(\vec{k}, \omega) = \sum_s \int \frac{d^3 p}{(2\pi \hbar)^3} \frac{\langle \vec{p} + \hbar \vec{k}/2 | \delta \hat{\rho}_{a,s}^\lambda(0) | \vec{p} - \hbar \vec{k}/2 \rangle}{\vec{v} \cdot \vec{k} - \omega}.
\tag{5}
$$

According to the basic postulate of the SMF approach, elements of the initial density matrix are uncorrelated Gaussian random numbers with zero mean values and with well-defined variances. In the semiclassical limit their variances are given by

$$
\overline{\langle \vec{p} + \hbar \vec{k}/2 | \delta \hat{\rho}_{a,s}^\lambda(0) | \vec{p} - \hbar \vec{k}/2 \rangle \langle \vec{p}' - \hbar \vec{k}'/2 | \delta \hat{\rho}_{b,s'}^\lambda(0) | \vec{p}' + \hbar \vec{k}'/2 \rangle} = \delta_{ab} \delta_{ss'} (2\pi \hbar)^6 \delta(\vec{p} - \vec{p}') \delta(\hbar \vec{k} - \hbar \vec{k}') f_a(\vec{p})[1 - f_a(\vec{p})].
\tag{6}
$$

The factor $\delta_{ab} \delta_{ss'}$ reflects the assumption that local density fluctuations in spin-isospin channels are uncorrelated in the initial state. In Eq. (4), F_0^{ab} and $\chi_a(\vec{k}, \omega)$ denote the zeroth-order Landau parameters and the Lindhard functions for protons and neutrons, respectively. Landau parameters are defined by the derivative of the mean-field potential energy with respect to the proton and neutron densities evaluated in the initial state, $F_0^{ab} = (\partial U_b / \partial \rho_a)_0$. The semiclassical expression of the Lindhard functions for neutrons and protons is given by

$$
\chi_a(\vec{k}, \omega) = 2 \int \frac{d^3 p}{(2\pi \hbar)^3} \frac{\vec{p} \cdot \hbar \vec{k}/m}{\hbar \omega - \vec{p} \cdot \hbar \vec{k}/m} \frac{\partial f_a(p)}{\partial \varepsilon}.
\tag{7}
$$

Here the factor 2 comes from spin summation, and $f_a(p)$ is the Fermi-Dirac factor for protons or neutrons in the initial state.

According to the method of one-sided Fourier transform [16,17], we can calculate the time evolution of the local density fluctuations by inverting Eq. (4) and taking the inverse Fourier transform to give

$$
\delta \rho_a^\lambda(\vec{k}, t) = -i \int_{-\infty + i\sigma}^{+\infty + i\sigma} \frac{d\omega}{2\pi} \frac{G_a^\lambda(\vec{k}, \omega)}{\varepsilon(\vec{k}, \omega)} e^{-i\omega t},
\tag{8}
$$

where the integral in the complex ω is carried out along a contour that passes above all singularities of the integrand. The quantity $G_a^\lambda(\vec{k}, \omega)$ in the integrand is given for neutrons and protons as

$$
\begin{pmatrix} G_n^\lambda(\vec{k}, \omega) \\ G_p^\lambda(\vec{k}, \omega) \end{pmatrix} = \begin{pmatrix} [1 + F_0^{pp} \chi_p(\vec{k}, \omega)] S_n^\lambda(\vec{k}, \omega) - F_0^{np} \chi_n(\vec{k}, \omega) S_p^\lambda(\vec{k}, \omega) \\ [1 + F_0^{nn} \chi_n(\vec{k}, \omega)] S_p^\lambda(\vec{k}, \omega) - F_0^{pn} \chi_p(\vec{k}, \omega) S_n^\lambda(\vec{k}, \omega) \end{pmatrix},
\tag{9}
$$

and $\varepsilon(\vec{k}, \omega)$ denotes the susceptibility

$$
\varepsilon(\vec{k}, \omega) = 1 + F_0^{nn} \chi_n(\vec{k}, \omega) + F_0^{pp} \chi_p(\vec{k}, \omega) + [F_0^{nn} F_0^{pp} - F_0^{np} F_0^{pn}] \chi_n(\vec{k}, \omega) \chi_p(\vec{k}, \omega).
\tag{10}
$$

As discussed in Ref. [15], it is possible to calculate the ω integral in Eq. (8) by choosing a contour as shown in Fig. 1 of Ref. [15]. There are collective poles determined by the roots of the dispersion relation, $\varepsilon(\vec{k}, \omega) = 0 \rightarrow \omega = \pm i \Gamma_k$. The collective poles play an important role in the early growth of density fluctuations in the spinodal region. However, the collective poles alone do not provide a complete description of the growth of density fluctuations. The collective poles alone do not even satisfy the initial conditions as pointed out in Ref. [14]. For a complete description, in addition to the collective poles, the effect of noncollective poles should be included into integral in Eq. (8). By calculating the angular integration in the Lindhard functions, it is easy to see that the integrand has a logarithmic singularity. The integrand in the complex ω plane is multivalued, therefore entire real ω axis is a branch cut. To calculate the integral in Eq. (8), we choose

the contour C, as shown in Fig. 1 of Ref. [15]. We exclude the real ω axis by drawing the contour from $+\infty$ to the origin just above the real ω axis, and after jumping from the first Riemann sheet to the second Riemann sheet at the origin, by drawing the contour just below the real ω axis from the origin to $+\infty$. The contour is completed with a large semicircle and by jumping from the second Riemann sheet to the first one at origin. As a result, we find that the integral in Eq. (8) can be expressed as

$$
\delta \rho_a^\lambda(\vec{k}, t) = \delta \rho_a^\lambda(P; \vec{k}, t) + \delta \rho_a^\lambda(C; \vec{k}, t),
\tag{11}
$$

where the pole (P) contribution and cut (C) contribution are given by

$$
\delta \rho_a^\lambda(P; \vec{k}, t) = -\sum_{\pm} \frac{G_a^\lambda(\vec{k}, \pm i \Gamma_k)}{\partial \varepsilon(\vec{k}, \omega) / \partial \omega |_{\omega = \pm i \Gamma_k}} e^{\pm \Gamma_k t},
\tag{12}
$$

and

$$
\begin{aligned}
&\delta\rho_a^\lambda(C;\vec{k},t)\\
&= -i \int_{-\infty}^{+\infty} \frac{d\omega}{2\pi}\left[\frac{G_a^\lambda(\vec{k},\omega+i\eta)}{\varepsilon(\vec{k},\omega+i\eta)} - \frac{G_a^\lambda(\vec{k},\omega-i\eta)}{\varepsilon(\vec{k},\omega-i\eta)}\right]e^{-i\omega t}.
\end{aligned}
$$
(13)

To investigate the development of spinodal instabilities a very useful quantity is the equal time correlation functions of local density fluctuations:

$$
\begin{aligned}
\sigma_{ab}(|\vec{r}-\vec{r}'|,t) &= \overline{\delta\rho_a^\lambda(\vec{r},t)\delta\rho_b^\lambda(\vec{r}',t)}\\
&= \int \frac{d^3k}{(2\pi)^3}e^{i\vec{k}\cdot(\vec{r}-\vec{r}')}\sigma_{ab}(\vec{k},t).
\end{aligned}
$$
(14)

Here the local nucleon density fluctuations $\delta\rho_a^\lambda(\vec{r}',t)$ are determined by the Fourier transform of $\delta\rho_a^\lambda(\vec{k},t)$, and the spectral intensity $\sigma_{ab}(\vec{k},t)$ of the correlation function is defined in terms of the variance of the Fourier transform of density fluctuations according to

$$
\sigma_{ab}(\vec{k},t)(2\pi)^3\delta(\vec{k}-\vec{k}') = \overline{\delta\rho_a^\lambda(\vec{k},t)\delta\rho_b^\lambda(-\vec{k}',t)}.
$$
(15)

In these expression, the bar indicates the average taken over the ensemble generated from the distribution of the initial fluctuations.

We can calculate the spectral intensity $\sigma_{ab}(\vec{k},t)$ by evaluating the ensemble averages using Eqs. (12) and (13) for the pole, $\delta\rho_a^\lambda(P;\vec{k},t)$, and the cut, $\delta\rho_a^\lambda(C;\vec{k},t)$, parts of the Fourier transform density fluctuations and using Eq. (6) for the initial fluctuations. As a result, the spectral intensity is expressed as

$$
\sigma_{ab}(\vec{k},t) = \sigma_{ab}(PP;\vec{k},t) + 2\sigma_{ab}(PC;\vec{k},t) + \sigma_{ab}(CC;\vec{k},t),
$$
(16)

where the first and last terms are due to pole and cut parts of the spectral intensity and the middle term denotes the mixed contribution. We briefly describe the derivation of the analytical expressions of the various terms in the spectral intensity in the long wavelength limit in the Appendix. The total spectral intensity is obtained by summing over the isospin components:

$$
\sigma(\vec{k},t) = \sigma_{pp}(\vec{k},t) + 2\sigma_{pn}(\vec{k},t) + \sigma_{nn}(\vec{k},t).
$$
(17)

The expression for the total correlation function of density fluctuations, $\sigma(|\vec{r}-\vec{r}'|,t)$, which is summed over isospin components, is determined by using the total spectral density $\sigma(\vec{k},t)$ in Eq. (14). Using Eq. (6), we can determine the initial condition of the spectral density $\sigma(\vec{k},0)$, which must be equal to the right-hand side of Eq. (18) at time $t = 0$. This leads to a nontrivial sum rule:

$$
\begin{aligned}
&\sum_{p,n} \int 2\frac{d^3p}{(2\pi\hbar)^3} f_a(\vec{p})[1-f_a(\vec{p})]\\
&= \sigma_{pp}(\vec{k},0) + 2\sigma_{pn}(\vec{k},0) + \sigma_{nn}(\vec{k},0).
\end{aligned}
$$
(18)

III. RESULTS OF CALCULATIONS

In numerical calculations, we employ the effective Skyrme potential of Ref. [4]:

$$
\begin{aligned}
U_a(\rho_n,\rho_p) &= A\left(\frac{\rho}{\rho_0}\right) + B\left(\frac{\rho}{\rho_0}\right)^{\alpha+1} + C\left(\frac{\rho'}{\rho_0}\right)\tau_a\\
&\quad + \frac{1}{2}\frac{dC}{d\rho}\frac{\rho'^2}{\rho_0} - D\Delta\rho + D'\Delta\rho'\tau_a,
\end{aligned}
$$
(19)

where $\rho = \rho_n + \rho_p$ and $\rho' = \rho_n - \rho_p$ are the total and relative densities, and $\tau_a = +1$ for neutrons and $\tau_a = -1$ for protons. The parameters $A = -356.8$ MeV, $B = +303.9$ MeV, $\alpha = 1/6$, and $D = +130.0$ MeV fm^5 are adjusted to reproduce the saturation properties of nuclear matter: the binding energy $\varepsilon_0 = 15.7$ MeV per nucleon, zero pressure at the saturation density $\rho_0 = 0.16$ fm^{-3}, compressibility coefficient $K = 201$ MeV, and the surface energy coefficient in the Weizsacker mass formula $a_{\text{surf}} = 18.6$ MeV. The magnitude of the parameter $D' = +34$ MeV fm^5 is close to the magnitude given by the SkM* [18]. The symmetry energy coefficient is
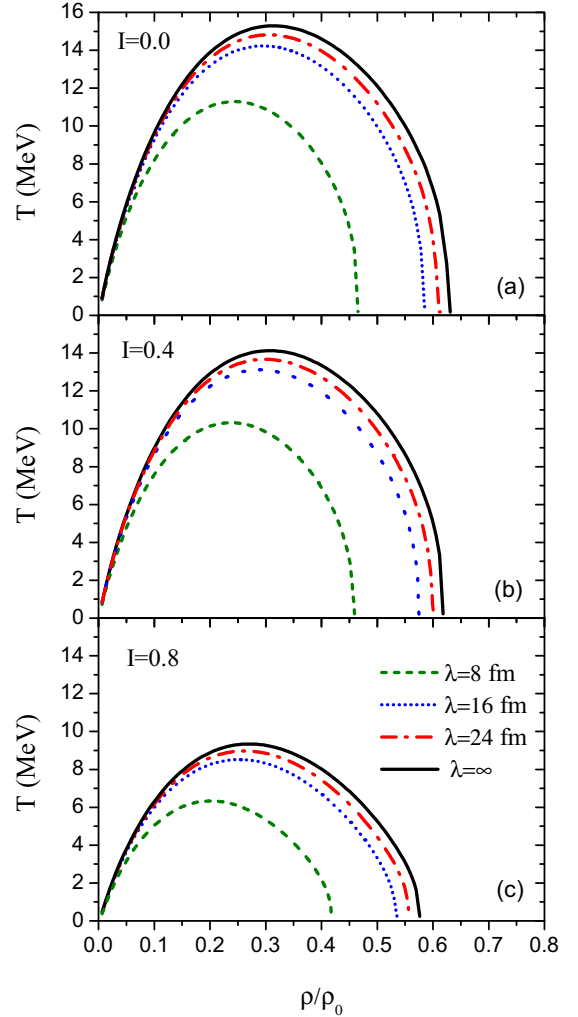

FIG. 1. (Color online) Phase diagram in the density-temperature plane for different wavelengths corresponding to the potential given by Eq. (19).

$C(\rho) = C_1 - C_2(\rho/\rho_0)^\alpha$ with $C_1 = +124.9$ MeV and $C_2 = +93.5$ MeV. These values for the symmetry energy coefficient in the Weizsacker mass formula give $a_{sym} = \varepsilon_F(\rho_0)/3 + C(\rho_0)/2 = 36.9/3 + 31.4/2 = 28.0$ MeV. We define the initial charge asymmetry as $I = (\rho_n - \rho_n)/\rho$.

Figure 1 shows phase diagrams for different charge asymmetries corresponding to different wavelengths in the temperature-density plane. These diagrams indicate the boundaries of spinodal unstable regions for different wavelengths, starting from the uppermost boundary for $\lambda = \infty$. The critical temperatures corresponding to this effective Skyrme potential, which depend on the initial charge asymmetries $I = 0.0$, $I = 0.4$, and $I = 0.8$, are given by $T_c = 15$ MeV, $T_c = 14$ MeV and $T_c = 10$ MeV, respectively. The critical temperatures occur approximately around the same initial density, $\rho = 0.3\rho_0$. We notice that, consistent with earlier calculations [1], the spinodal instability region shrinks for increasing values of charge asymmetry. Neutron-rich matter with $I = 0.8$ and $T = 1.0$ MeV approximately corresponds to the structure

of the crust of neutron stars. Under these conditions, the limiting spinodal boundary occurs at nucleon density around $\rho = 0.55\rho_0$, which is consistent with the result found in Ref. [19]. We pick a reference state located at the center of the spinodal region with an initial density of $\rho = 0.3\rho_0$ and calculate the equal time correlation function of density fluctuations at two different temperatures: $T = 1.0$ MeV and $T = 5.0$ MeV. In Figs. 2 and 3, we plot the total spectral intensity $\sigma(\vec{k},t)$ of correlation functions as a function of wave number k at time $t = 40$ fm/c for two different temperatures and three different initial charge asymmetries. At each initial charge asymmetry and temperature, the upper limit of the wave number range k_{max} is determined by the condition that the inverse growth rate of the mode vanishes, $\Gamma_k = 0$. Dashed, dash-dotted, and solid lines indicate the results of calculations in Eq. (17) with pole contributions $\sigma_{ab}(PP;\vec{k},t)$ only, with cut contributions only, and the total of all terms, respectively. The cut contributions include the cut-cut contribution $\sigma_{ab}(CC;\vec{k},t)$ and the cross terms due to pole-cut parts $2\sigma_{ab}(PC;\vec{k},t)$. From
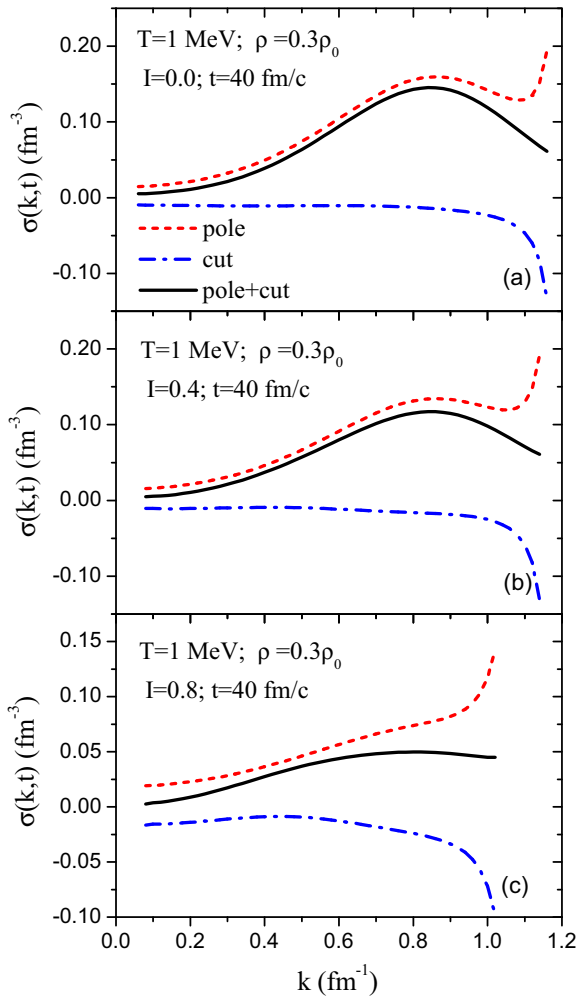

FIG. 2. (Color online) Spectral intensity of the correlation function as a function of wave number at initial density $\rho = 0.3\rho_0$ fm^{-3} at time $t = 40$ fm/c at temperature $T = 1$ MeV for three different charge asymmetries. Dotted, dashed-dotted, and solid lines are the results of pole, cut, and total contributions, respectively.
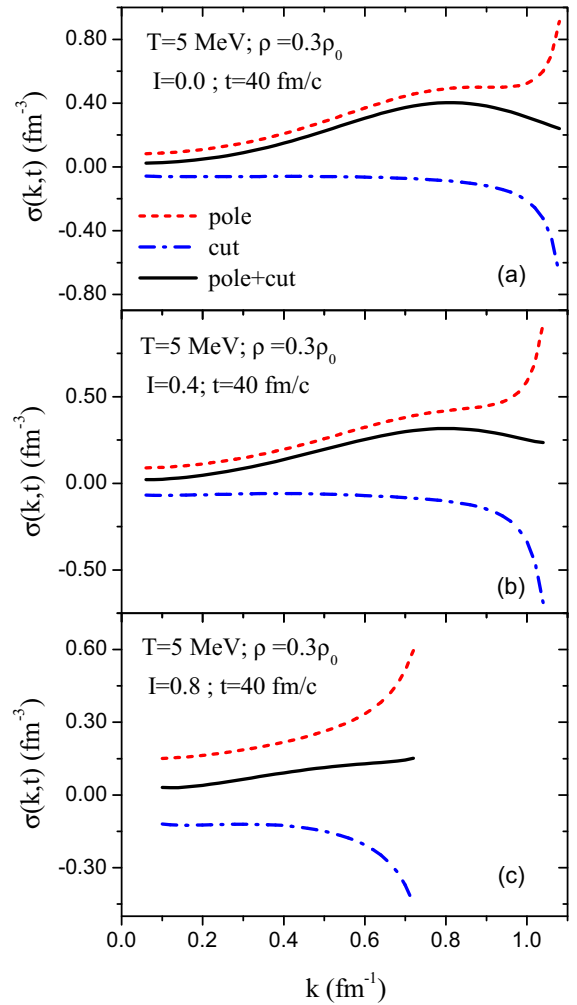
FIG. 3. (Color online) Spectral intensity of the correlation function as a function of wave number at initial density $\rho = 0.3\rho_0$ fm^{-3} at time $t = 40$ fm/c at temperature $T = 5$ MeV for three different charge asymmetries. Dotted, dashed-dotted, and solid lines are the results of pole, cut, and total contributions, respectively.
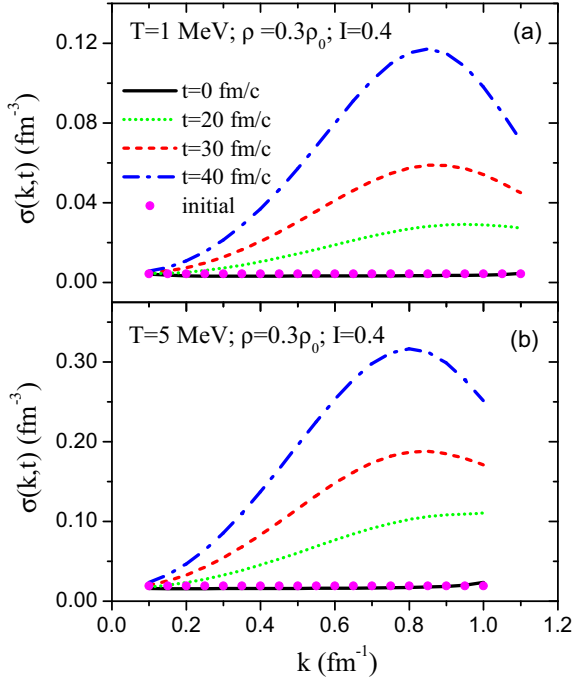
FIG. 4. (Color online) Spectral intensity of the correlation function as a function of wave number at initial density $\rho = 0.3\rho_0$ fm^{-3} and charge asymmetry $I = 0.4$ for different times at temperature $T = 1$ MeV (a) and $T = 5$ MeV (b). Dots on the solid lines at times $t = 0$ represent the initial conditions.

FIG. 5. (Color online) Density correlation function as a function of distance between two space locations $x = |\vec{r} - \vec{r}'|$ for initial density $\rho = 0.3\rho_0$ fm^{-3} and different charge asymmetries at temperature $T = 1$ MeV at times $t = 20, 30$, and 40 fm/c.

these figures, similar to the charge symmetric matter, we make two important observations for each value of the charge asymmetry. Cut terms make an important negative contribution during the early phase of growth, hence slowing down the growth of instabilities. During later times, collective poles dominate the growth of density fluctuations, and the cut terms representing the effects of noncollective poles do not grow in time, as discussed in earlier studies [1]. The second point that we note is that both pole and cut contributions have divergent behavior with opposite signs, as the wave number approaches its upper limit, $k \rightarrow k_{max}$. These divergent behaviors cancel out each other to produce a nice regular behavior of the spectral intensity as a function of wave number. Figure 4 shows the total spectral intensity of the correlation function $\sigma(\vec{k}, t)$ for a typical charge asymmetry, $I = 0.4$, as a function of wave number k at different times for initial temperatures $T = 1.0$ MeV and $T = 5.0$ MeV. We observe that the spectral intensity, which includes pole and cut contributions, clearly exhibits the growth of the initial density fluctuations. The initial value of the spectral intensity at time $t = 0$ indicated by the solid line is obtained by numerical calculations of the pole-pole terms $\sigma_{ab}(PP; \vec{k}, t = 0)$, the cut-cut terms $\sigma_{ab}(CC; \vec{k}, t = 0)$, and the pole-cut terms $2\sigma_{ab}(PC; \vec{k}, t = 0)$. On the other hand, the solid circles on this line are calculated by the initial conditions located on the left -hand side of Eq. (18). Nice agreement of both sides reflects the validity of the highly nontrivial sum rule presented by Eq. (18).

Figure 5 shows the equal time correlation functions $\sigma(|\vec{r} - \vec{r}'|, t)$ of the total density fluctuations as a function distance
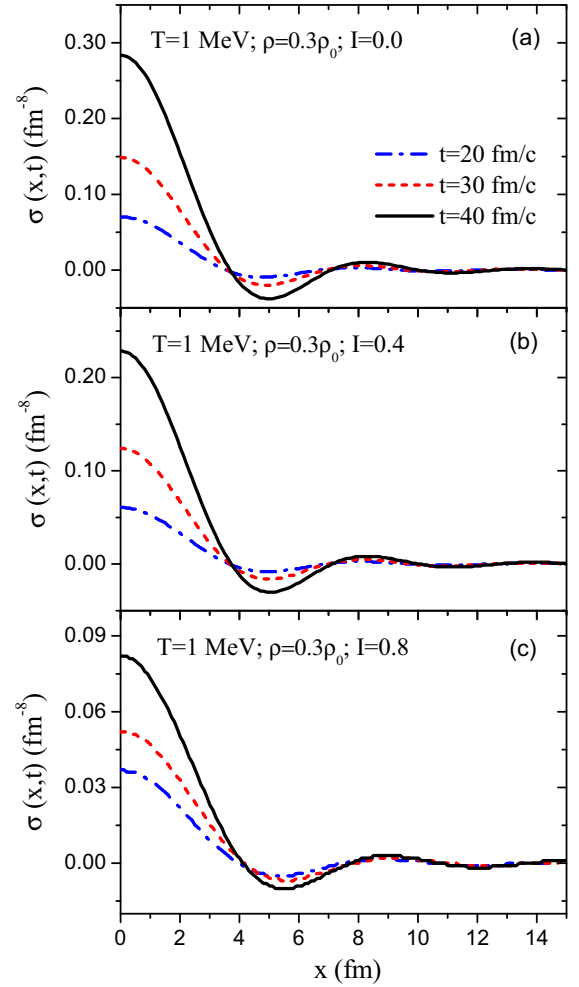
of two space locations $x = |\vec{r} - \vec{r}'|$ at the initial density $\rho = 0.3\rho_0$ and temperature $T = 1.0$ MeV for three different charge asymmetries. The density correlation functions are calculated with complete spectral intensities shown by solid lines in Fig. 5, and the results are plotted at three different times, $t = 20, 30$, and 40 fm/c. In Fig. 6, these correlation functions are plotted at temperature $T = 5.0$ MeV. The growth and organization of the correlation function describes the initial phase of the condensation mechanism. To recognize the condensation mechanism, it is useful to introduce the correlation length x_C as the width of the correlation function at half maximum. The correlation length provides a measure for the size of condensing droplets during the growth of fluctuations. In the correlation volume $\Delta V_C = 4\pi x_C^3/3$, the variance of local density fluctuations at time t is approximately given by $\sigma(x_C, t)$. The number of nucleons in each correlation volume fluctuates with a dispersion, $\Delta A_C = \Delta V_C \sqrt{\sigma(x_C, t)}$. As a result, the total nucleon number in each correlation volume fluctuates approximately within the range $\Delta A_0 - \Delta A_C \leqslant \Delta A \leqslant \Delta A_0 + \Delta A_C$, where $\Delta A_0 = \Delta V_C \rho_0$ denotes
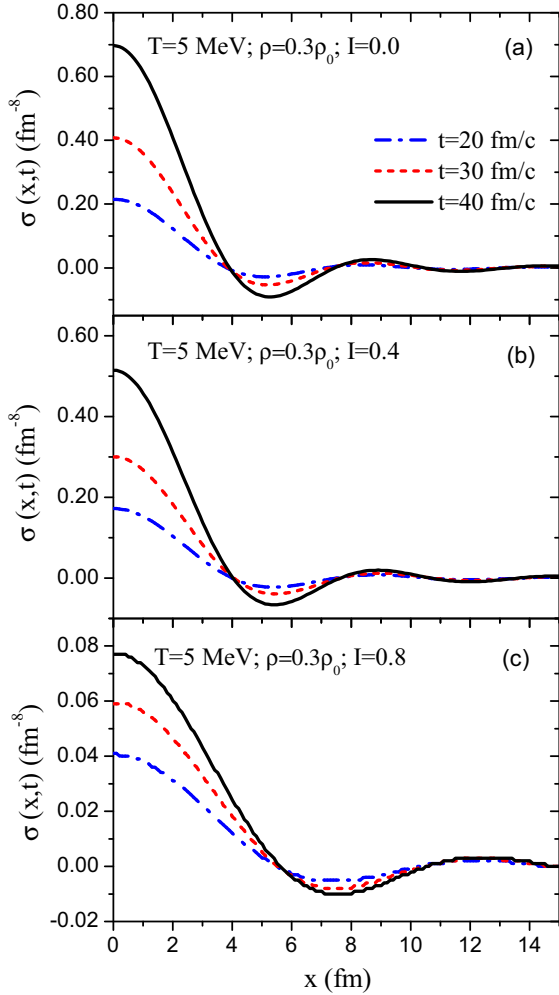
FIG. 6. (Color online) Density correlation function as a function of distance between two space locations $x = |\vec{r} - \vec{r}'|$ for initial density $\rho = 0.3\rho_0$ fm^{-3} and different charge asymmetries at temperature $T = 5$ MeV at times $t = 20$, 30, and 40 fm/c.

the number of nucleons in the initial uniform state. As seen from Figs. 5 and 6, the correlation length is not very sensitive to the temperature and time evolution, but depends on the initial charge asymmetry. For example, at temperature $T = 5.0$ MeV and the initial charge asymmetry $I = 0.4$, the correlation length is about $x_C = 3.0$ fm. In this case, the magnitude of the dispersion of density fluctuations at time $t = 30$ fm/c is about $\sqrt{\sigma(x_C,t)} = 0.04$ fm^{-3}. Consequently, the number of nucleons in the correlation volume approximately fluctuates in the range of $1 \leqslant \Delta A \leqslant 9$. From this analysis, we observe

that the spinodal decomposition indeed provides a dynamical mechanism for the liquid-gas phase transition. In the linear response approach, we can only recognize the early phase of the transition. To describe the full phase transition, we need to carry out long time simulations, which has not been done in this study.

IV. CONCLUSIONS

As a continuation of a previous work, we investigate the early growth of density fluctuations in charge asymmetric nuclear matter in the basis of the SMF approach. In the linear response framework, employing the method of one-sided Fourier transform, it is possible to carry out nearly analytical treatment of the correlation function of density fluctuations. The density correlation function provides very useful information about the initial phase of the liquid-gas phase transformation of the system. The method of one-sided Fourier transform involves a contour integration in the complex frequency plane. In earlier investigations, this contour integral is evaluated by keeping only effects of the collective poles associated with unstable collective modes. This approximation, although it describes the growth of density fluctuations in a satisfactory manner, has important drawbacks. It does not satisfy the initial conditions and furthermore leads to a divergent behavior as the wave numbers approach their upper limits. In this work, we consider charge asymmetric nuclear matter in a nonrelativistic framework of the SMF approach. We calculate the correlation function of density fluctuations including the effects of collective poles and noncollective poles in terms of the cut contribution in the complex frequency plane. The cut contribution slows down the exponential growth of the pole contributions. It also has divergent behaviors with opposite signs, as wave numbers approach their upper limits. As a result divergent behaviors of pole and contributions cancel out each other to produce a nice regular behavior of the spectral intensity as a function of wave number. This allows us to have a complete description of the correlation function of density fluctuations in the linear response regime. Furthermore, exact calculations of the correlation functions satisfy the initial conditions expressed by a highly nontrivial sum rule.

APPENDIX

As seen in Eq. (17), there are three parts in the spectral intensity $\sigma_{ab}(\vec{k},t)$: the pole-pole part, the cut-cut part, and the mixed cut-pole part. The pole-pole part is

$$\tilde{\sigma}_{ab}(PP;\vec{k},t) = \frac{E_{ab}^+}{|[\partial \varepsilon(\vec{k},\omega)/\partial \omega]_{\omega=i\Gamma_k}|^2}(e^{+2\Gamma_k t} + e^{-2\Gamma_k t}) + \frac{2E_{ab}^-}{|[\partial \varepsilon(\vec{k},\omega)/\partial \omega]_{\omega=i\Gamma_k}|^2}, \tag{A1}$$

where the quantities $E_{ab}^{\mp}$ for neutrons and protons are given by

$$E_{nn}^{\mp} = \left[1 + F_0^{pp}\chi_p\right]^2 I_n^{\mp} + \left[F_0^{np}\chi_n\right]^2 I_p^{\mp}, \tag{A2}$$

$$E_{pp}^{\mp} = \left[1 + F_0^{nn}\chi_n\right]^2 I_p^{\mp} + \left[F_0^{pn}\chi_p\right]^2 I_n^{\mp}, \tag{A3}$$

and

$$E_{np}^{\mp} = -\left(1 + F_0^{pp}\chi_p\right)F_0^{pn}\chi_p I_n^{\mp} - \left(1 + F_0^{nn}\chi_n\right)F_0^{np}\chi_n I_p^{\mp}, \tag{A4}$$

with

$$I_a^{\mp} = 2\int \frac{d^3p}{(2\pi\,\hbar)^3} \frac{[(\Gamma_k)^2 \mp (\vec{p}\cdot\vec{k}/m)^2]}{[(\Gamma_k)^2 + (\vec{p}\cdot\vec{k}/m)^2]^2} f_a(\vec{p})[1 - f_a(\vec{p})]. \tag{A5}$$

The pole-pole contributions have the same expressions as we had in our previous investigation in the semiclassical framework [16]. The cut-cut part has four terms:

$$\tilde{\sigma}_{ab}(CC;\vec{k},t) = A_{ab}^+(\vec{k},t) + \tilde{A}_{ab}^+(\vec{k},t) + \tilde{A}_{ab}^-(\vec{k},t) + A_{ab}^-(\vec{k},t). \tag{A6}$$

The first and last terms come from the square of the first and second terms in Eq. (13) and involve double integrations over ω and ω'. The diagonal and off-diagonal parts in the isospin space are

$$\begin{pmatrix} A_{nn}^{\mp}(\vec{k},t) \\ A_{pp}^{\mp}(\vec{k},t) \end{pmatrix} = \int_{-\infty}^{+\infty}\frac{d\omega}{2\pi}\int_{-\infty}^{+\infty}\frac{d\omega'}{2\pi}\frac{e^{-i(\omega+\omega')t}}{\omega+\omega'\mp 2i\eta}\begin{pmatrix} W_{nn}^{\mp} & V_{np}^{\mp} \\ V_{pn}^{\mp} & W_{pp}^{\mp} \end{pmatrix} \otimes \begin{pmatrix} \frac{\phi_n(\omega\mp i\eta)+\phi_n(\omega'\mp i\eta)}{\varepsilon(\omega\mp i\eta)\varepsilon(\omega'\mp i\eta)} \\ \frac{\phi_p(\omega\mp i\eta)+\phi_p(\omega'\mp i\eta)}{\varepsilon(\omega\mp i\eta)\varepsilon(\omega'\mp i\eta)} \end{pmatrix} \tag{A7}$$

and

$$A_{pn}^{\mp}(\vec{k},t) = -\int_{-\infty}^{+\infty}\frac{dw}{2\pi}\int_{-\infty}^{+\infty}\frac{dw'}{2\pi}\frac{e^{-i(\omega+\omega')t}}{\omega+\omega'\mp 2i\eta}(W_{pn}^{\mp} \quad V_{nn}^{\mp}) \otimes \begin{pmatrix} \frac{\phi_n(\omega\mp i\eta)+\phi_n(\omega'\mp i\eta)}{\varepsilon(\omega\mp i\eta)\varepsilon(\omega'\mp i\eta)} \\ \frac{\phi_p(\omega\mp i\eta)+\phi_p(\omega'\mp i\eta)}{\varepsilon(\omega\mp i\eta)\varepsilon(\omega'\mp i\eta)} \end{pmatrix}. \tag{A8}$$

In these expressions and below, the symbol $\otimes$ denotes the matrix multiplication. The double integrals in $A_{ab}^{\mp}(\vec{k},t)$ contain the principle value and the delta function contributions, which are identified using the identity $1/(\omega+\omega'\mp 2i\eta) = P(1/\omega+\omega')\pm i\pi\delta(\omega+\omega')$. The elements of W and V matrices are given by

$$\begin{pmatrix} W_{nn}^{\mp} & V_{np}^{\mp} \\ V_{pn}^{\mp} & W_{pp}^{\mp} \end{pmatrix} = \begin{pmatrix} \left(1+F_0^{pp}\chi_p^{\mp}\right)\left(1+F_0^{pp}\chi_p'^{\mp}\right) & \left(F_0^{np}\right)^2\chi_n^{\mp}\chi_n'^{\mp} \\ \left(F_0^{pn}\right)^2\chi_p^{\mp}\chi_p'^{\mp} & \left(1+F_0^{nn}\chi_n^{\mp}\right)\left(1+F_0^{nn}\chi_n'^{\mp}\right) \end{pmatrix} \tag{A9}$$

and

$$\begin{pmatrix} W_{pn}^{\mp} \\ V_{nn}^{\mp} \end{pmatrix} = \begin{pmatrix} F_0^{pn}\chi_p^{\mp}\left(1+F_0^{pp}\chi_p'^{\mp}\right) \\ \left(1+F_0^{nn}\chi_n^{\mp}\right)F_0^{np}\chi_n'^{\mp} \end{pmatrix}. \tag{A10}$$

In these expressions and also below, we use the shorthand notation $\chi_a^{\mp} = \chi_a(\vec{k},\omega\mp i\eta)$ and $\chi_a'^{\mp} = \chi_a(\vec{k},\omega'\mp i\eta)$, and the quantity $\phi_a(\omega\mp i\eta)$ is defined as

$$\phi_a(\omega\mp i\eta) = 2\int_{-\infty}^{+\infty}\frac{d^3p}{(2\pi\,\hbar)^3}f_a(\vec{p})[1-f_a(\vec{p})]\frac{1}{\vec{p}\cdot\vec{k}/m-(\omega\mp i\eta)}. \tag{A11}$$

There are contributions coming from the cross terms in the square of Eq. (13), which are indicated by the second and third terms in Eq. (A6). These terms also involves double integrations over ω and ω' and have structures similar to that of $A_{ab}^{\mp}(\vec{k},t)$:

$$\begin{pmatrix} \tilde{A}_{nn}^{\mp}(\vec{k},t) \\ \tilde{A}_{pp}^{\mp}(\vec{k},t) \end{pmatrix} = -\int_{-\infty}^{+\infty}\frac{d\omega}{2\pi}\int_{-\infty}^{+\infty}\frac{d\omega'}{2\pi}\frac{e^{-i(\omega+\omega')t}}{\omega+\omega'}\begin{pmatrix} \tilde{W}_{nn}^{\mp} & \tilde{V}_{np}^{\mp} \\ \tilde{V}_{pn}^{\mp} & \tilde{W}_{pp}^{\mp} \end{pmatrix} \otimes \begin{pmatrix} \frac{\phi_n(\omega\mp i\eta)+\phi_n(\omega'\pm i\eta)}{\varepsilon(\omega\mp i\eta)\varepsilon(\omega'\pm i\eta)} \\ \frac{\phi_p(\omega\mp i\eta)+\phi_p(\omega'\pm i\eta)}{\varepsilon(\omega\mp i\eta)\varepsilon(\omega'\pm i\eta)} \end{pmatrix} \tag{A12}$$

and

$$\tilde{A}_{pn}^{\pm}(\vec{k},t) = \int_{-\infty}^{+\infty}\frac{dw}{2\pi}\int_{-\infty}^{+\infty}\frac{dw'}{2\pi}\frac{e^{-i(\omega+\omega')t}}{\omega+\omega'}(\tilde{W}_{pn}^{\mp} \quad \tilde{V}_{nn}^{\mp}) \otimes \begin{pmatrix} \frac{\phi_n(\omega\pm i\eta)+\phi_n(\omega'\mp i\eta)}{\varepsilon(\omega\pm i\eta)\varepsilon(\omega'\mp i\eta)} \\ \frac{\phi_p(\omega\pm i\eta)+\phi_p(\omega'\mp i\eta)}{\varepsilon(\omega\pm i\eta)\varepsilon(\omega'\mp i\eta)} \end{pmatrix}. \tag{A13}$$

The integrand in $\tilde{A}_{ab}^{\mp}(\vec{k},t)$, in contrast to its appearance, is a well-behaved function, because when $\omega' = -\omega$, the nominator is also zero and therefore the ratio $[\phi(\omega\mp i\eta)+\phi(\omega'\pm i\eta)]/(\omega+\omega')$ becomes finite. Here, the elements of $\tilde{W}$ and $\tilde{V}$ matrices are

given by

$$
\begin{pmatrix} \tilde{W}_{nn}^{\mp} & \tilde{V}_{np}^{\mp} \\ \tilde{V}_{pn}^{\mp} & \tilde{W}_{pp}^{\mp} \end{pmatrix} = \begin{pmatrix} \left(1 + F_0^{pp}\chi_p^{\mp}\right)\left(1 + F_0^{pp}\chi_p'^{\pm}\right) & \left(F_0^{np}\right)^2 \chi_n^{\mp} \chi_n'^{\pm} \\ \left(F_0^{pn}\right)^2 \chi_p^{\mp} \chi_p'^{\pm} & \left(1 + F_0^{nn}\chi_n^{\mp}\right)\left(1 + F_0^{nn}\chi_n'^{\pm}\right) \end{pmatrix}
\tag{A14}
$$

and

$$
\begin{pmatrix} W_{pn}^{\mp} \\ V_{nn}^{\mp} \end{pmatrix} = \begin{pmatrix} F_0^{pn}\chi_p^{\pm}\left(1 + F_0^{pp}\chi_p'^{\mp}\right) \\ \left(1 + F_0^{nn}\chi_p^{\pm}\right)F_0^{np}\chi_n'^{\mp} \end{pmatrix}.
\tag{A15}
$$

In spectral density, the pole-cut contribution also has four terms:

$$
\tilde{\sigma}_{ab}(PC;\vec{k},t) = B_{ab}^+(\vec{k},t) + \tilde{B}_{ab}^+(\vec{k},t) + \tilde{B}_{ab}^-(\vec{k},t) + B_{ab}^-(\vec{k},t).
\tag{A16}
$$

The isospin matrix elements of the first and the last term are given by

$$
\begin{pmatrix} B_{nn}^{\mp}(\vec{k},t) \\ B_{pp}^{\mp}(\vec{k},t) \end{pmatrix} = \frac{\pm ie^{\mp\Gamma t}}{\partial\varepsilon/\partial\omega|_{\omega=\mp i\Gamma}} \int_{-\infty}^{+\infty} \frac{d\omega}{2\pi} \frac{e^{-i\omega t}}{\omega\mp i\Gamma} \begin{pmatrix} X_{nn}^{\mp} & Y_{np}^{\mp} \\ Y_{pn}^{\mp} & X_{pp}^{\mp} \end{pmatrix} \otimes \begin{pmatrix} \frac{\phi_n(\mp i\Gamma)+\phi_n(\omega\mp i\eta)}{\varepsilon(\omega\mp i\eta)} \\ \frac{\phi_p(\mp i\Gamma)+\phi_p(\omega\mp i\eta)}{\varepsilon(\omega\mp i\eta)} \end{pmatrix}
\tag{A17}
$$

and

$$
B_{pn}^{\mp}(\vec{k},t) = \frac{\mp ie^{\mp\Gamma t}}{\partial\varepsilon/\partial\omega|_{\omega=\mp i\Gamma}} \int_{-\infty}^{+\infty} \frac{d\omega}{2\pi} \frac{e^{-i\omega t}}{\omega\mp i\Gamma} (X_{pn}^{\mp} \quad Y_{nn}^{\mp}) \otimes \begin{pmatrix} \frac{\phi_n(\mp i\Gamma_k)+\phi_n(\omega\mp i\eta)}{\varepsilon(\omega\mp i\eta)} \\ \frac{\phi_p(\mp i\Gamma_k)+\phi_p(\omega\mp i\eta)}{\varepsilon(\omega\mp i\eta)} \end{pmatrix}.
\tag{A18}
$$

Here, we use the shorthand notation $\phi_a(\mp i\Gamma) = \phi_a(\vec{k},\omega = \mp i\Gamma)$, we ignore the label k in Γ_k for simplicity, and the elements of X and Y matrices are given by

$$
\begin{pmatrix} X_{nn}^{\mp} & Y_{np}^{\mp} \\ Y_{pn}^{\mp} & X_{pp}^{\mp} \end{pmatrix} = \begin{pmatrix} \left(1 + F_0^{pp}\chi_p^{\mp i\Gamma}\right)\left(1 + F_0^{pp}\chi_p^{\mp}\right) & \left(F_0^{np}\right)^2 \chi_n^{\mp i\Gamma} \chi_n^{\mp} \\ \left(F_0^{pn}\right)^2 \chi_p^{\mp i\Gamma} \chi_p^{\mp} & \left(1 + F_0^{nn}\chi_n^{\mp i\Gamma}\right)\left(1 + F_0^{nn}\chi_n^{\mp}\right) \end{pmatrix}
\tag{A19}
$$

and

$$
\begin{pmatrix} X_{pn}^{\mp} \\ Y_{nn}^{\mp} \end{pmatrix} = \begin{pmatrix} F_0^{pn}\chi_p^{\mp i\Gamma}\left(1 + F_0^{pp}\chi_p^{\mp}\right) \\ \left(1 + F_0^{nn}\chi_n^{\mp i\Gamma}\right)F_0^{np}\chi_n^{\mp} \end{pmatrix},
\tag{A20}
$$

where $\chi_a^{\mp i\Gamma} = \chi_a(\vec{k},\omega = \mp i\Gamma)$. The second and third terms involve an integral over ω and have structures similar to that of $B_{ab}^{\mp}(\vec{k},t)$:

$$
\begin{pmatrix} \tilde{B}_{nn}^{\mp}(\vec{k},t) \\ \tilde{B}_{pp}^{\mp}(\vec{k},t) \end{pmatrix} = \frac{\mp ie^{\mp\Gamma t}}{\partial\varepsilon/\partial\omega|_{\omega=\mp i\Gamma}} \int_{-\infty}^{+\infty} \frac{d\omega}{2\pi} \frac{e^{-i\omega t}}{\omega\mp i\Gamma} \begin{pmatrix} \tilde{X}_{nn}^{\mp} & \tilde{Y}_{np}^{\mp} \\ \tilde{Y}_{pn}^{\mp} & \tilde{X}_{pp}^{\mp} \end{pmatrix} \otimes \begin{pmatrix} \frac{\phi_n(\mp i\Gamma)+\phi_n(\omega\pm i\eta)}{\varepsilon(\omega\pm i\eta)} \\ \frac{\phi_p(\mp i\Gamma)+\phi_p(\omega\pm i\eta)}{\varepsilon(\omega\pm i\eta)} \end{pmatrix}
\tag{A21}
$$

and

$$
\tilde{B}_{pn}^{\mp}(\vec{k},t) = \frac{\pm ie^{\mp\Gamma t}}{\partial\varepsilon/\partial\omega|_{\omega=\mp i\Gamma}} \int_{-\infty}^{+\infty} \frac{d\omega}{2\pi} \frac{e^{-i\omega t}}{\omega\mp i\Gamma} (\tilde{X}_{pn}^{\mp} \quad \tilde{Y}_{nn}^{\mp}) \otimes \begin{pmatrix} \frac{\phi_n(\mp i\Gamma)+\phi_n(\omega\pm i\eta)}{\varepsilon(\omega\pm i\eta)} \\ \frac{\phi_p(\mp i\Gamma)+\phi_p(\omega\pm i\eta)}{\varepsilon(\omega\pm i\eta)} \end{pmatrix}.
\tag{A22}
$$

The elements of $\tilde{X}$ and $\tilde{Y}$ matrices are given by

$$
\begin{pmatrix} \tilde{X}_{nn}^{\mp} & \tilde{Y}_{np}^{\mp} \\ \tilde{Y}_{pn}^{\mp} & \tilde{X}_{pp}^{\mp} \end{pmatrix} = \begin{pmatrix} \left(1 + F_0^{pp}\chi_p^{\mp i\Gamma}\right)\left(1 + F_0^{pp}\chi_p^{\pm}\right) & \left(F_0^{np}\right)^2 \chi_n^{\mp i\Gamma} \chi_n^{\pm} \\ \left(F_0^{pn}\right)^2 \chi_p^{\mp i\Gamma} \chi_p^{\pm} & \left(1 + F_0^{nn}\chi_n^{\mp i\Gamma}\right)\left(1 + F_0^{nn}\chi_n^{\pm}\right) \end{pmatrix}
\tag{A23}
$$

and

$$
\begin{pmatrix} \tilde{X}_{pn}^{\mp} \\ \tilde{Y}_{nn}^{\mp} \end{pmatrix} = \begin{pmatrix} F_0^{pn}\chi_p^{\mp i\Gamma}\left(1 + F_0^{pp}\chi_p^{\pm}\right) \\ \left(1 + F_0^{nn}\chi_n^{\mp i\Gamma}\right)F_0^{np}\chi_n^{\pm} \end{pmatrix}.
\tag{A24}
$$

[1] Ph. Chomaz, M. Colonna, and J. Randrup, Phys. Rep. **389**, 263 (2004).

[2] S. Ayik and C. Gregoire, Phys. Lett. B **212**, 269 (1988); Nucl. Phys. A **513**, 187 (1990).

[3] J. Randrup and B. Remaud, Nucl. Phys. A **514**, 339 (1990).

[4] V. Baran, M. Colonna, M. Di Tora, and A. B. Larionov, Nucl. Phys. A **632**, 287 (1998).

[5] Y. Abe, S. Ayik, P.-G. Reinhard, and E. Suraud, Phys. Rep. **275**, 49 (1996).

[6] M. Tohyama and A. S. Umar, Phys. Lett. B **549**, 72 (2002).

[7] D. Lacroix, S. Ayik, and Ph. Chomaz, Prog. Part. Nucl. Phys. **52**, 497 (2004).

[8] S. Ayik, Phys. Lett. B **658**, 174 (2008).

[9] S. Ayik, N. Er, O. Yilmaz, and A. Gokalp, Nucl. Phys. A **812**, 44 (2008).

[10] S. Ayik, O. Yilmaz, N. Er, A. Gokalp, and P. Ring, Phys. Rev. C **80**, 034613 (2009).

[11] S. Ayik, O. Yilmaz, F. Acar, B. Danisman, N. Er, and A. Gokalp, Nucl. Phys. A **859**, 73 (2011).

[12] O. Yilmaz, S. Ayik, and A. Gokalp, Eur. Phys. J. A **47**, 123 (2011).

[13] O. Yilmaz, S. Ayik, F. Acar, S. Saatci, and A. Gokalp, Eur. Phys. J. A **49**, 33 (2013).

[14] P. Bozek, Phys. Lett. B **383**, 121 (1996).

[15] O. Yilmaz, S. Ayik, F. Acar, and A. Gokalp, Phys. Rev. C **91**, 014605 (2015).

[16] E. M. Lifshitz and L. P. Pitaevskii, *Physical Kinetics* (Pergamon, Oxford, 1981).

[17] H. Heiselberg, C. J. Pethick, and D. G. Ravenhall, Phys. Rev. Lett. **61**, 818 (1988).

[18] H. Krivine, J. Trainer, and O. Bohigas, Nucl. Phys. A **336**, 155 (1980).

[19] J. Xu and C. M. Ko, Phys. Rev. C **82**, 044311 (2010).